Homogeneous Catalysis

DOI: 10.1002/ange.201406415

Gold(I) Catalysis at Extreme Concentrations Inside Self-Assembled Nanospheres**

*Rafael Gramage-Doria, Joeri Hessels, Stefan H. A. M. Leenders, Oliver Tröppner, Maximilian Dürr, Ivana Ivanović-Burmazović, and Joost N. H. Reek**

Abstract: *Homogeneous transition-metal catalysis is a crucial technology for the sustainable preparation of valuable chemicals. The catalyst concentration is usually kept as low as possible, typically at mM or μM levels, and the effect of high catalyst concentration is hardly exploited because of solubility issues and the inherent unfavorable catalyst/substrate ratio. Herein, a self-assembly strategy is reported which leads to local catalyst concentrations ranging from 0.05 M to 1.1 M, inside well-defined nanospheres, whilst the overall catalyst concentration in solution remains at the conventional mM levels. We disclose that only at this high concentration, the gold(I) chloride is reactive and shows high selectivity in intramolecular C–O and C–C bond-forming cyclization reactions.*

Transition-metal catalysis plays an extremely important role in the synthesis of chemicals relevant for pharmacology, biology, agrochemistry, materials science, and petrochemistry.[1] It allows the preparation of valuable molecules from readily available bulk chemicals in an atom-economic and sustainable manner.[2] It also enables the construction of sophisticated molecules in more efficient manners, thus simplifying synthetic routes towards the desired target molecules.[3] In the past decades several tools to control the activity and selectivity of transition-metal catalysts have been developed, and have mostly focused on the ligands which together with the metal form the active complex.[4,5] More recently, enzyme-inspired approaches have been explored, thus providing excellent tools to control the second coordination sphere around the transition-metal complex.[6] Various examples demonstrate that the use of a second coordination sphere can lead to activities and selectivities which are not accessible by traditional approaches.[7] The operational modes of these second spheres are many, including the precise orientation of the substrate at the metal center[8] and controlling the local pH value.[9]

What all these catalysts have in common is that they are employed in a limited concentration window, typically between 10^{-6} M and 10^{-3} M. At these concentrations the catalysts generally dissolve well and a large excess of substrate can be added to achieve high turnover numbers without running into limitations of substrate solubility. From a reactivity point of view, however, it is interesting to also explore extremely high concentrations of catalyst as new reactivity patterns may evolve through, for example, metal cooperativity effects. We realized that if one would like to apply molar concentrations of catalyst, this can only be achieved by devising systems in which the "local catalyst concentration" is high, whereas the overall catalyst concentration in solution is still around the commonly used 10^{-3} M (Figure 1), thus still allowing high turnover numbers to be achieved. Fujita et al. have developed appealing strategies to form nanosized molecular spheres ($M_{12}L_{24}$) which form by self-assembly of 24 ditopic nitrogen ligands and 12 palladium metals.[10] Functionalization of the ditopic ligand is explored intensively as a tool for both inner- and outer-sphere decoration. As such, various functional groups have been enclosed within the $M_{12}L_{24}$ spheres.[11] These systems are well suited to explore catalysis at high local catalyst concentration, as we estimated that enclosing 24 metal complexes within this sphere would lead to a local 1.1 M concentration. Herein we report an approach based on the assembly of $M_{12}L_{24}$ spheres using novel ditopic nitrogen ligands in which the local gold-complex concentration can be tuned from 1.1 M to 0.05 M. We have chosen gold(I) catalysis because of its increasing relevance for organic synthesis[12] and the observation that cooperativity between metals plays a role in some of the proposed mechanisms.[13]

To prepare novel gold-containing spheres we first prepared the ditopic building blocks **A** and **B** (Figure 2). **A** is utilized with a [R_3PAuCl] (R = aryl) unit which is attached by a spacer, whereas **B** contains an acetate functional group instead. All building blocks were obtained according to standard synthetic procedures and fully characterized (see the Supporting Information). Next, we studied by nuclear magnetic resonance (NMR), diffusion-ordered NMR (DOSY), and cryo-spray ionization mass spectroscopy (CSI-MS) the typical formation of $M_{12}L_{24}$ spheres upon mixing **A** (or **B**)

[*] Dr. R. Gramage-Doria, J. Hessels, S. H. A. M. Leenders, Prof. Dr. J. N. H. Reek
Homogeneous, Supramolecular and Bio-Inspired Catalysis, Van't Hoff Institute for Molecular Sciences, University of Amsterdam
Science Park 904, 1098XH Amsterdam (The Netherlands)
E-mail: j.n.h.reek@uva.nl
Dr. O. Tröppner, M. Dürr, Prof. Dr. I. Ivanović-Burmazović
Lehrstuhl für Bioanorganische Chemie, Department Chemie und Pharmazie, Friedrich-Alexander-Universitaet Erlangen
Egerlandstrasse 3, 91058 Erlangen (Germany)

[**] Financial support was provided by the University of Amsterdam, The Netherlands Organization for Scientific Research-Chemical Sciences (NWO-TOP to J.N.H.R.), and by the National Research School for Catalysis. NWO is acknowledged for a Rubicon grant to R.G.-D. I.I.-B., O.T., and M.D. gratefully acknowledge support through the "Solar Technologies Go Hybride" initiative of the State of Bavaria. Prof. Dr. Bas de Bruin, Dr. Jarl I. van der Vlugt, Dr. Gunnar W. Klau, and M.Sc. Louis J. Dijkstra are also acknowledged for helpful discussions.

Supporting information for this article is available on the WWW under http://dx.doi.org/10.1002/anie.201406415.

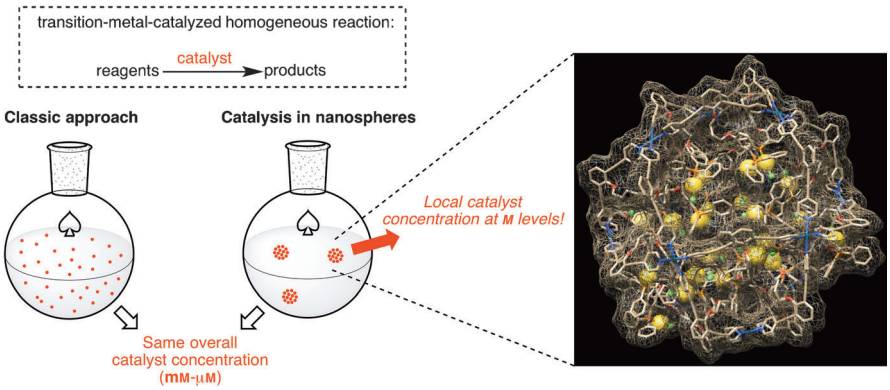

Figure 1. New approach allowing the use of high local catalyst concentration (1 M), whereas the average catalyst concentration is in the usual 10^{-3}–10^{-6} M range.

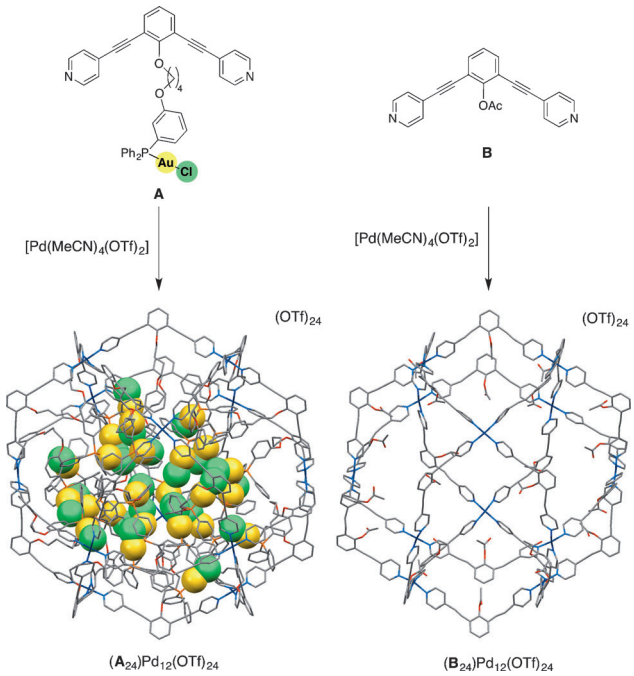

Figure 2. Building blocks **A** (left) and **B** (right) employed in this study. PM3-Spartan-modeled supramolecular spheres derived from **A** and **B**. Tf = trifluoromethanesulfonyl.

with $[Pd(MeCN)_4(OTf)_2]$ as the appropriate palladium precursor (Figure 2).

The ^{1}H NMR spectra clearly show the typical shift of the pyridine protons, thus indicating coordination to palladium, and the simplicity of the spectra indicate the formation of highly symmetric structures consistent with $\mathbf{A}_{24}Pd_{12}$ and $\mathbf{B}_{24}Pd_{12}$ spheres (see Figures S22 and S37 in the Supporting Information). DOSY studies revealed that the structures formed in solution are about 5 nm in diameter (see Figure S30 in the Supporting Information), which is in line with the data reported by Fujita et al. for these types of structures.[11a] Final evidence for the formation of well-defined sphere structures came from CSI-MS analysis. For $\mathbf{B}_{24}Pd_{12}$ a clean spectrum was obtained with peaks displaying the expected isotopic pattern at 2013.4220, 1704.5132, 1472.8300, 1292.6317, 1148.3730, 1030.4342, and 932.1523 belonging respectively to $[M-m(OTf)]^{m+}$ ($m=6$ to 12; see Figures S39–S46 in the Supporting Information). Also, for $\mathbf{A}_{24}Pd_{12}$ we obtained a clean CSI-MS spectrum which clearly indicates the formation of the spheres with 24 gold complexes inside, as evidenced by peaks observed at 2686.5668, 2403.0168, 2171.0194, 1977.6041, and 1814.0993 corresponding to $[M-m((OTf)]^{m+}$ ($m=9$ to 13; see Figures S31–S36 in the Supporting Information). The $^{31}P\{^1H\}$ NMR spectrum of the $\mathbf{A}_{24}Pd_{12}$ sphere displayed only a small downfield shift observed upon self-assembly formation ($\Delta\delta =$ 0.4 ppm with respect to **A**; see Figure S25 in the Supporting Information), thus indicating that the phosphine gold [AuCl] complex is compatible with the self-assembly process. $^{19}F\{^1H\}$ NMR spectroscopy indicates, as expected, the presence of noncoordinated triflate anions (see Figures S27 and S38 in the Supporting Information).

Having established that the $\mathbf{A}_{24}Pd_{12}$ and $\mathbf{B}_{24}Pd_{12}$ spheres can be prepared by simple self-assembly of the building blocks, we were interested in the preparation of the mixed spheres using different ratios of **A** and **B** in the presence of palladium(II) cations (Figure 3). Since there is no clear strong

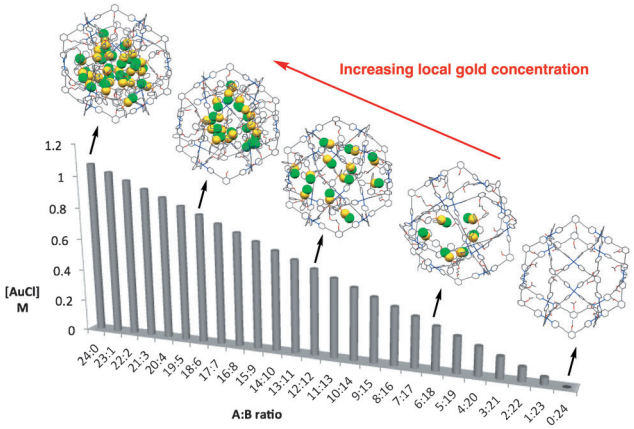

Figure 3. Estimated local [AuCl] concentration inside a given sphere as a function of the ratio **A** and **B** used to form the assembly, and five typical examples in which the number of gold atoms clearly varies (top).

driving force for the self-sorted formation of spheres, the use of mixtures leads to a local dilution of the gold concentration. We estimated that the local gold concentration of gold complexes by dilution in these spheres could be controlled between within the range between 0.05 M and 1.1 M, by just mixing different ratios of building blocks **A** and **B** during the assembly formation (Figure 3). The formation of a statistical mixture of spheres should follow a binomial distribution of $(\mathbf{A}_n\mathbf{B}_{24-n})Pd_{12}(OTf)_{24}$ (see Section S8 in the Supporting Information), and for the various ratios of **A** and **B** these distributions are displayed in Figure 4. For example, at the 12:12 ratio of **A**/**B**, the predicted distribution with a maximum at the 1:1 ratio is shown in green.

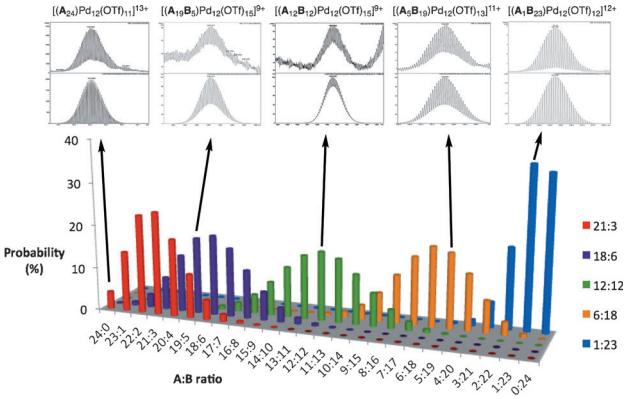

Figure 4. Top: Illustrative peaks in the CSI-MS spectra [measured (top)spectrum versus simulated spectrum (bottom)] of selected spheres $(\mathbf{A}_n\mathbf{B}_{24-n})Pd_{12}(OTf)_{24}$ present in the statistical mixture. Bottom: Binomial distribution of spheres $(\mathbf{A}_n\mathbf{B}_{24-n})Pd_{12}(OTf)_{24}$ formed at different **A**/**B** ratios: 1:23 (blue, 6:18 (orange), 12:12 (green), 18:6 (violet), 21:3 (red) with a palladium(II) precursor.

The formation of spheres based on mixtures of the building blocks **A** and **B** (different ratios 1:23, 6:18, 12:12, 18:6 and 21:3) in the presence of $[Pd(MeCN)_4(OTf)_2]$ was studied by CSI-MS and NMR spectroscopy. Indeed, ^{1}H NMR spectra clearly show that all pyridine protons were involved in palladium coordination and that the formed structures are symmetric, which is in line with sphere formation. The simplicity of the ^{1}H NMR spectra indicates that the presence of different amounts of gold inside the sphere does not change the NMR signature of the outer framework. Also, in these experiments the phosphine coordination to the [AuCl] complex remains intact, as is confirmed by $^{31}P\{^1H\}$ NMR spectroscopy. As expected from statistical mixtures of spheres in which the number of gold complexes varies, the CSI-MS spectra of the solutions are more complex than the parent $\mathbf{A}_{24}Pd_{12}$ and $\mathbf{B}_{24}Pd_{12}$ spheres, but the expected peaks of the various spheres in the mixtures could be identified in all experiments with various ratios of **A** and **B** [(peaks at m/z $[M-m((OTf)]^{m+}$ $(m=7$ to 13)]. The expected isotopic profiles belonging to the main spheres that should form according to the mathematical model were most prominent, and typical examples are displayed in Figure 4 (for more details see the Supporting Information). For example, the CSI-MS spectrum of the mixture formed with a ratio of **A**/**B** = 1:23 clearly shows the peaks with the expected isotopic profiles at m/z values for $[M-m((OTf)]^{m+}$ $(m=7$ to 13) belonging to $(\mathbf{A}_0\mathbf{B}_{24})Pd_{12}(OTf)_{24}$, $(\mathbf{A}_1\mathbf{B}_{23})Pd_{12}(OTf)_{24}$, and $(\mathbf{A}_2\mathbf{B}_{22})Pd_{12}(OTf)_{24}$. The same features were found when mixing **A** and **B** at ratios 6:18, 12:12, 18:6, and 21:3 with the palladium(II) precursor (see Tables S1–S5 in the Supporting Information), and illustrative peaks including the calculated isotope patterns are displayed in Figure 4. Importantly, with this strategy in hand we can create spheres in which we control the *local* concentration of gold complexes (Figure 3 and section S9 in the Supporting Information), which allows, for the first time, a study of the effect of extremely high concentrations of catalyst on its reactivity.

With these gold(I)-containing spheres[14] $(\mathbf{A}_n\mathbf{B}_{24-n})Pd_{12}(OTf)_{24}$ in hand we explored the effect of local catalyst concentration in the hydroalkoxylation of the γ-allenol **1**, a typical gold-mediated transformation, in which **1** can react in an intramolecular fashion to give either the product **2** as a five-membered ring or **3** as a six-membered ring (Table 1).

Table 1: Hydroalkoxylation of the allenol **1**.[a]

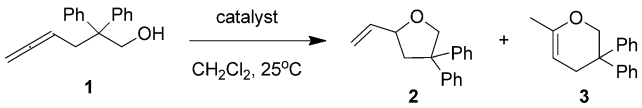

1 **2** **3**

Entry	Catalyst $\mathbf{A}_A\mathbf{B}_BPd_{12}(OTf)_{24}$ (**A**/**B** ratio)	mol% (mol% **A**)	Overall [AuCl] [mM][b]	Local [AuCl] [M][c]	Yield **2** [%][d]	TON
1	1:23	48 (48)	5	0.05	0 (–)	0
2	6:18	8 (48)	5	0.27	10 (–)	0.21
3	12:12	4 (48)	5	0.54	37 (–)	0.76
4	18:6	2.7 (48)	5	0.80	55 (50)	1.13
5	21:3	2.3 (48)	5	0.94	82 (80)	1.69
6	24:0	2 (48)	5	1.07	90 (88)	1.86

[a] [**1**] = 10.4 mM, (see the Supporting Information for details).
[b] Overall concentration of [AuCl] in the reaction mixture. [c] Average concentration of [AuCl] within the spheres according to Figure 3.
[d] Calculated yield (after 12 h) as determined by ^{1}H NMR spectroscopy. Value within parentheses is that of the yield of the isolated product after column chromatography; reactions performed 2–3 times.

The selectivity of this reaction is determined by the attack of the hydroxy nucleophile group on one of the carbon atoms of the allene group.[13d] In the first experiments, different sets of self-assembled spheres with local gold concentrations varying between 0.05 M and 1.1 M were used as catalysts, while keeping the overall gold concentration in solution at 5 mM (Table 1). When the local gold concentration was higher than 0.27 M (ratio **A**/**B** > 6:18) product formation was observed, which increases with the local concentration (Table 1, entries 2–6).[15] With the highest local concentration the yield of the isolated product was 88%. Remarkably, usually the AuCl complexes become active only after abstraction of the chloride, but at these high concentrations in the spheres the AuCl complexes are already active. Indeed, control experiments employing free AuCl complexes do not show any conversion under these reaction conditions. This is the case for gold complexes based on building block **A** as well as for benchmark Ph_3PAuCl, that is no conversion even with 24 mol% of Ph_3PAuCl at 1.1 M concentration (see Table S12 in the Supporting Information). Next to the unusual activity of the AuCl complexes, we also found that all active catalysts were selectively forming the small cyclic compound **2**.

The formation of **2** was monitored over time by ^{1}H NMR spectroscopy (see Figure S122 in the Supporting Information), from which the turnover numbers (TON) and initial turnover frequencies (TOF_{ini}) were calculated (Table 1 and Figure 5). These results clearly indicate that the catalyst activity increases with the local gold concentration (overall gold concentration was the same in all experiments), that is, at high **A**/**B** ratios, with the highest activity observed for $\mathbf{A}_{24}Pd_{12}(OTf)_{24}$ ([AuCl] ca. 1.1 M; Figures 3 and 5). The TOF_{ini} and TON values were increased by further optimization of the parameters (see Table S10 in the Supporting

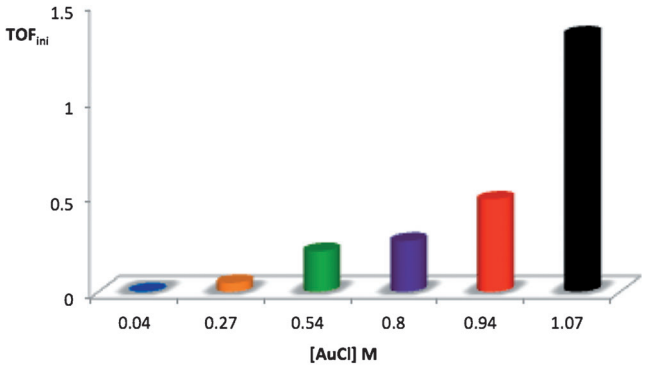

Figure 5. Plot of TOF_{ini} calculated at 15% conversion versus the local gold concentration within each sphere; the overall gold concentration is 5 mM in all experiments. Data are obtained by fitting the initial part of the reaction profiles of the different reactions [**A**/**B** = 1:23 (blue), 6:18 (orange), 12:12 (green), 18:6 (violet), 21:3 (red), 24:0 (black); see the Supporting Information for details].

Information), that is, application of higher temperatures (90 °C in toluene as solvent) and decreasing catalyst loading. Under these reaction conditions a TON of 67 and TOF_{ini} of 55 h^{-1} were reached using $\mathbf{A}_{24}Pd_{12}(OTf)_{24}$ at 0.03125 mol% (0.75 mol% of AuCl; see Figure S125 in the Supporting Information).

After having established the unusual reactivity of these spheres, we explored the activity of $\mathbf{A}_{24}Pd_{12}(OTf)_{24}$ in the gold(I)-catalyzed intramolecular cycloisomerization of the less reactive substrate 1,6-enyne **4** [Eq. (1)], which typically produces two products when traditional cationic gold complexes are applied.[16] As expected, the reaction proceeds more slowly than the reaction shown in Table 1, and at room temperature in the presence of 2 mol% $\mathbf{A}_{24}Pd_{12}(OTf)_{24}$ (48 mol% AuCl) no conversion was obtained. Interestingly at 40 °C, 45% conversion was reached, and at 90 °C full conversion was obtained after 12 hours (95% yield). Under reaction conditions in which the overall gold concentration was 1.19×10^{-4} M (sphere concentration 1.25×10^{-6} M) the reaction performed smoothly at 90 °C, leading to 19.3% conversion and implying a TON of 26 with respect to the gold concentration (see Table S11 in the Supporting Information). Interestingly, $\mathbf{A}_{24}Pd_{12}(OTf)_{24}$ produces only **5** as the product, which is unusual as there are only limited examples with in situ generated cationic gold(I) species complexes which are selective.[16c,17]

The origin of the activity at high gold-chloride concentration inside the sphere is puzzling, and control experiments using Ph_3PAuCl or **A** applied at the same high concentration [1.1 M, the concentration within sphere $\mathbf{A}_{24}Pd_{12}(OTf)_{24}$] did not show conversion, thus suggesting that next to the high local gold concentration, other factors play a role. We hypothesized that the limited freedom of the individual gold complexes inside the $\mathbf{A}_{24}Pd_{12}(OTf)_{24}$ sphere leads to a further preorganization which may be required for the formation of the final active species. Interestingly, UV/Vis measurements performed on $\mathbf{A}_{24}Pd_{12}(OTf)_{24}$ show a broad shoulder at about $\lambda = 315$ nm (Figure 6 and section S7 in the Supporting Information), thus suggesting the formation of higher-order

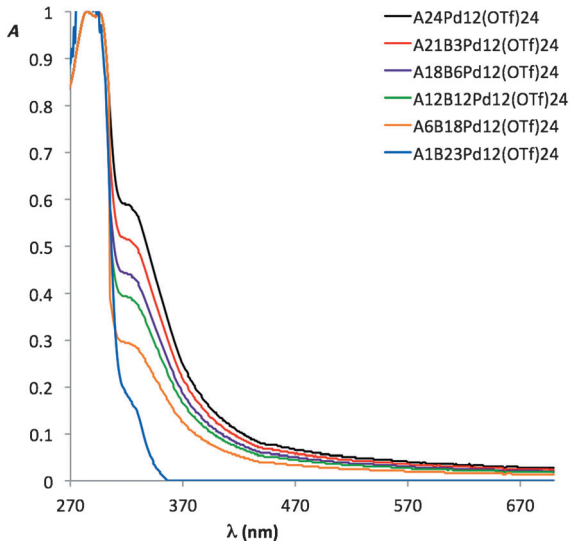

Figure 6. Normalized UV/Vis spectra of solutions of $\mathbf{A}_n\mathbf{B}_{24-n}Pd_{12}(OTf)_{24}$ in acetonitrile at room temperature showing an increased band at $\lambda = 315$ nm, indicative of d^{10}–d^{10} aurophilic interactions at high local concentrations.

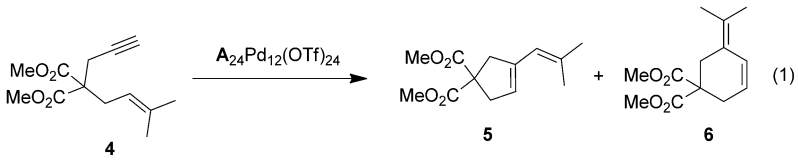

complexes which experience d^{10}–d^{10} aurophilic interactions.[18] Upon diluting the local gold-chloride concentration within the spheres, by using lower **A**/**B** ratios during the sphere formation, the shoulder at about $\lambda = 315$ nm decreases in intensity (Figure 6; see Figure S121 in the Supporting Information). This change shows that the concentration of complexes that display d^{10}–d^{10} aurophilic interactions increases the high local gold concentration, which correlates with the activity observed in catalysis (see Table S9 in the Supporting Information). In line with the inactivity of the Ph_3PAuCl complex, we did not observe the shoulders that typically indicate d^{10}–d^{10} aurophilic interactions, even at 1.1 M (see Figure S120 in the Supporting Information).[19]

Next to these findings, we observed only the peaks belonging to active spheres $\mathbf{A}_n\mathbf{B}_{24-n}Pd_{12}(OTf)_{24}$ and inactive building block **A** in the $^{31}P\{^1H\}$ NMR spectra during the catalytic reactions.[15] Most interestingly, if a lot of product is formed, the sphere disassembled completely, with the remaining building block **A** (the gold(I) chloride complex) as the only species, thus supporting the formation of the catalytically active species only at high concentration within the sphere. This outcome suggests that either a) the chloride dissociation to generate an active cationic gold species, facilitated by Au···Au interactions is reversible and too fast to be detected on NMR time scale or b) the chloride does not

dissociate and Au···Au interactions occur to form a multinuclear $(P\text{-}Au\text{-}Cl)_n$ complex that is responsible for the activity.

In conclusion, we report here a self-assembly strategy to prepare nanosized molecular spheres with an extremely high metal-complex concentration inside. The local gold-chloride concentration can be controlled between 0.05 and 1.1 M by just mixing the various bifunctional building blocks used for sphere formation in different ratios. Importantly, the overall catalyst concentration in solution can be kept identical and at the usual 10^{-6}–10^{-3} M range. This control allows, for the first time, a thorough investigation of the reactivity at catalyst concentrations at the molar level, a dimension underexplored in homogeneous catalysis. The high local catalyst concentration turns an inactive AuCl complex into an active system. Next to this unusual reactivity displayed by the gold chloride complexes, the nanospheres also displays high selectivities in intramolecular cycloisomerization reactions. As the self-assembly strategy is simple and based on accessible building blocks, the approach is likely widely applicable and new reactivity can be uncovered by exploring high concentration catalysis.

Received: June 27, 2014
Revised: July 18, 2014
Published online: September 12, 2014

Keywords: gold · homogeneous catalysis · metal–metal interactions · nanostructures · supramolecular chemistry

[1] B. Cornils, W. A. Herrmann in *Applied Homogeneous Catalysis with Organometallic Compounds*, 2ednd edWiley-VCH, Weinheim, **2002**.

[2] a) R. A. Sheldon, I. Arends, U. Hanefeld in *Green Chemistry and Catalysis*, Wiley-VCH, Weinheim, **2007**; b) G. Rothenberg in *Catalysis*, Wiley-VCH, Weinheim, **2008**; c) R. Franke, D. Selent, A. Boerner, *Chem. Rev.* **2012**, *112*, 5675 – 5732.

[3] M. Beller, C. Bolm in *Transition Metals for Organic Synthesis*, Wiley-VCH, Weinheim, **2004**.

[4] J. F. Hartwig in *Organotransition Metal Chemistry: From Bonding to Catalysis*, University Science Books, Sausalito, CA, **2009**.

[5] P. W. N. M. van Leeuwen in *Homogeneous Catalysis: Understanding the Art*, Kluwer Academic Publishers, Dordrecht, **2004**.

[6] For reviews, see: a) D. M. Vriezema, M. Comellas Aragones, J. A. A. W. Elemans, J. J. L. M. Cornelissen, A. E. Rowan, R. J. M. Nolte, *Chem. Rev.* **2005**, *105*, 1445 – 1490; b) T. Koblenz, J. Wassenaar, J. N. H. Reek, *Chem. Soc. Rev.* **2008**, *37*, 247 – 262; c) M. J. Wiester, P. A. Ulmann, C. A. Mirkin, *Angew. Chem. Int. Ed.* **2011**, *50*, 114 – 137; *Angew. Chem.* **2011**, *123*, 118 – 142; d) J. Meeuwissen, J. N. H. Reek, *Nat. Chem.* **2010**, *2*, 615 – 621; e) Z. Dong, Q. Luo, J. Liu, *Chem. Soc. Rev.* **2012**, *41*, 7890 – 7908.

[7] For a review, see: P. Dydio, J. N. H. Reek, *Chem. Sci.* **2014**, *5*, 2135.

[8] a) S. Das, C. D. Incarvito, R. H. Crabtree, G. W. Brudvig, *Science* **2006**, *312*, 1941 – 1943; b) P. Dydio, W. I. Dzik, M. Lutz, B. de Bruin, J. N. H. Reek, *Angew. Chem. Int. Ed.* **2011**, *50*, 396 – 400; *Angew. Chem.* **2011**, *123*, 416 – 420; c) P. Dydio, J. N. H. Reek, *Angew. Chem. Int. Ed.* **2013**, *52*, 3878 – 3882; *Angew. Chem.* **2013**, *125*, 3970 – 3974; d) V. Bocokic, A. Kalkan, M. Lutz, A. L. Spek, D. T. Gryko, J. N. H. Reek, *Nat. Commun.* **2013**, *4*, 2670.

[9] a) M. D. Pluth, R. G. Bergman, K. N. Raymond, *Science* **2007**, *316*, 85 – 88; b) M. D. Pluth, R. G. Bergman, K. N. Raymond, *J. Am. Chem. Soc.* **2007**, *129*, 11459 – 11467.

[10] M. Yoshizawa, J. K. Klosterman, M. Fujita, *Angew. Chem. Int. Ed.* **2009**, *48*, 3418 – 3438; *Angew. Chem.* **2009**, *121*, 3470 – 3490.

[11] a) K. Harris, D. Fujita, M. Fujita, *Chem. Commun.* **2013**, *49*, 6703 – 6712; b) K. Harris, Q.-F. Sun, S. Sato, M. Fujita, *J. Am. Chem. Soc.* **2013**, *135*, 12497 – 12499.

[12] a) A. S. K. Hashmi, F. D. Toste in *Modern Gold Catalyzed Synthesis*, Wiley-VCH, Weinheim, **2012**; b) A. S. K. Hashmi, G. J. Hutchings, *Angew. Chem. Int. Ed.* **2006**, *45*, 7896 – 7936; *Angew. Chem.* **2006**, *118*, 8064 – 8105.

[13] a) D. J. Gorin, F. D. Toste, *Nature* **2007**, *446*, 395 – 403; b) A. Gómez-Suárez, S. P. Nolan, *Angew. Chem. Int. Ed.* **2012**, *51*, 8156 – 8159; *Angew. Chem.* **2012**, *124*, 8278 – 8281; c) Z. Zhang, R. A. Widenhoefer, *Angew. Chem. Int. Ed.* **2007**, *46*, 283 – 285; *Angew. Chem.* **2007**, *119*, 287 – 289; d) Z. Zhang, C. Liu, R. E. Kinder, X. Han, H. Qian, R. A. Widenhoefer, *J. Am. Chem. Soc.* **2006**, *128*, 9066 – 9073.

[14] For examples on supramolecular encapsulation of single cationic gold(I) complexes and catalysis, see: a) Z. Wang, C. J. Brown, R. G. Bergman, K. N. Raymond, F. D. Toste, *J. Am. Chem. Soc.* **2011**, *133*, 7358 – 7360; b) A. Cavarzan, A. Scarso, P. Sgarbossa, G. Strukul, J. N. H. Reek, *J. Am. Chem. Soc.* **2011**, *133*, 2848 – 2851; c) Z. J. Wang, K. N. Clary, R. G. Bergman, K. N. Raymond, F. D. Toste, *Nat. Chem.* **2013**, *5*, 100 – 103; d) W. M. Hart-Cooper, K. N. Clary, F. D. Toste, R. G. Bergman, K. N. Raymond, *J. Am. Chem. Soc.* **2012**, *134*, 17873 – 17876; e) L. Adriaenssens, A. Escribano-Cuesta, A. Homs, A. M. Echavarren, P. Ballester, *Eur. J. Org. Chem.* **2013**, 1494 – 1500.

[15] Control experiments in which the isolated product **2** was added to a solution of the sphere $\mathbf{A}_{24}Pd_{12}$ show the appearance of peaks belonging to the building block **A**, presumably because of the coordination of **2** to palladium.

[16] a) C. Bartolomé, Z. Ramiro, P. Pérez-Galán, C. Bour, M. Raducan, A. M. Echavarren, P. Espinet, *Inorg. Chem.* **2008**, *47*, 11391 – 11397; b) C. Bartolomé, Z. Ramiro, D. Garcia-Cuadrado, P. Pérez-Galán, M. Raducan, C. Bour, A. M. Echavarren, P. Espinet, *Organometallics* **2010**, *29*, 951 – 956; c) M. Raducan, M. Moreno, C. Bour, A. M. Echavarren, *Chem. Commun.* **2012**, *48*, 52 – 54; d) S. Ito, S. Kusano, N. Morita, K. Mikami, M. Yoshifuji, *J. Organomet. Chem.* **2010**, *695*, 291 – 296; e) M. Raducan, C. Rodriguez-Escrich, X. C. Cambeiro, E. C. Escudero-Adan, M. A. Pericas, A. M. Echavarren, *Chem. Commun.* **2011**, *47*, 4893 – 4895; f) M. Guitet, P. Zhang, F. Marcelo, C. Tugny, J. Jimenez-Barbero, O. Buriez, C. Amatore, V. Mouries-Mansuy, J.-P. Goddard, L. Fensterbank, Y. Zhang, S. Roland, M. Menand, M. Sollogoub, *Angew. Chem. Int. Ed.* **2013**, *52*, 7213 – 7218; *Angew. Chem.* **2013**, *125*, 7354 – 7359.

[17] a) C. Nieto-Oberhuber, M. P. Munoz, S. Lopez, E. Jimenez-Nunez, C. Nevado, E. Herrero-Gomez, M. Raducan, A. M. Echavarren, *Chem. Eur. J.* **2006**, *12*, 1677 – 1693; b) C. Nieto-Oberhuber, S. Lopez, M. Paz Munoz, D. J. Cardenas, E. Bunuel, C. Nevado, A. M. Echavarren, *Angew. Chem. Int. Ed.* **2005**, *44*, 6146 – 6148; *Angew. Chem.* **2005**, *117*, 6302 – 6304.

[18] a) S. Cauteruccio, A. Loos, A. Bossi, M. C. Blanco Jaimes, D. Dova, F. Rominger, S. Prager, A. Dreuw, E. Licandro, A. S. K. Hashmi, *Inorg. Chem.* **2013**, *52*, 7995 – 8004; b) C. Sarcher, A. Luehl, F. C. Falk, S. Lebedkin, M. Kuehn, C. Wang, J. Paradies, M. M. Kappes, W. Klopper, P. W. Roesky, *Eur. J. Inorg. Chem.* **2012**, 5033 – 5042.

[19] a) J. Oliver-Meseguer, A. Leyva-Perez, S. I. Al-Resayes, A. Corma, *Chem. Commun.* **2013**, *49*, 7782 – 7784; b) Unfortunately, since the shoulder at about $\lambda = 315$ nm overlaps with the main band of the spheres, fluorescence studies were unsatisfactory.